Published in final edited form as:
Virology. 2008 September 15; 379(1): 78–86. doi:10.1016/j.virol.2008.05.030.

A more precise HIV integration assay designed to detect small differences finds lower levels of integrated DNA in HAART treated patients

Jianqing J. Yu[1], **Te Lang Wu**[2], **Megan Liszewski**[1], **Jihong Dai**[1], **William J. Swiggard**[3], **Clifford Baytop**[1], **Ian Frank**[4], **Bruce L. Levine**[1], **Wei Yang**[5], **Theodore Theodosopoulos**[6], and **Una O'Doherty**[1,*]

1*Department of Pathology and Laboratory Medicine, Division of Transfusion Medicine, University of Pennsylvania, Philadelphia, Pennsylvania*

2*Department of Microbiology, University of Pennsylvania, Philadelphia, Pennsylvania*

3*Cooley Dickinson Hospital, Northampton, Massachusetts; Department of Medicine*

4*Division of Infectious Diseases, Hospital of the University of Pennsylvania, Philadelphia, Pennsylvania*

5*Center for Clinical Epidemiology and Biostatistics, University of Pennsylvania, Philadelphia, Pennsylvania*

6*IKOS Research, UK*

Abstract

Many studies report the level of total viral DNA in HIV-infected patients, but few studies report the level of integrated DNA. It is important to measure integrated DNA in HIV-infected patients because the information could shed light on the effectiveness of antiretroviral therapy, especially intensified therapy, when viral loads may remain undetectable. In order to develop an integration assay for patient samples we enhanced the sensitivity of our prior integration assay. To do this, we exploited a technique that we developed, called repetitive sampling, and optimized reaction conditions for rare event detection, rather than large dynamic range. We also redesigned our primers to match more conserved regions of HIV. The result is a new, sensitive, quantitative assay that allows us to measure integrated DNA in HIV-infected patients. When we applied our integration assay to patient PBMCs, we found that use of HAART is associated with reduced levels of integrated DNA.

Keywords

HIV; integration; latency; persistence; reservoirs; HAART; antiretroviral therapy; eradication; ongoing replication; intensification

*To whom correspondence should be addressed. Una O'Doherty, 3620 HamiltonWalk, JMB, Philadelphia, PA 19104, unao@mail.med.upenn.edu, 215-573-7273, 215-572-2348.

Introduction

Integration is a central step in the HIV life cycle: it is required for efficient transcription of the genome, for replication, and for establishment of reservoirs. Given that integration is essential for viral survival in the host, it is important to monitor the level of integrated DNA. In addition, unintegrated DNA is only transcribed at low levels (Brussel and Sonigo, 2004; Nakajima, Lu, and Engelman, 2001; Wu and Marsh, 2001; Wu and Marsh, 2003a; Wu and Marsh, 2003b), and is likely to contribute little to productive HIV infection (Nakajima, Lu, and Engelman, 2001). Thus, it may be important to distinguish between integrated an unintegrated HIV DNA. However, measuring integration accurately in patient samples is difficult for two reasons. First, in HIV-infected individuals, unintegrated DNA is present in excess over integrated DNA and so routine PCR does not distinguish unintegrated from integrated DNA. Second, the level of integration in HIV-infected individuals is low and detection is a further challenge since only a fraction of integration events are detectable because of the widely distributed integration sites (Agosto et al., 2007). While many studies have reported the level of total viral DNA in cells from HIV-infected individuals (Brenchley et al., 2004; Burgard et al., 2000; Debiaggi et al., 2000; Douek et al., 2002; Gibellini et al., 2004; Jubault et al., 1998; Kabamba-Mukadi et al., 2005; Kostrikis et al., 2002; Lillo et al., 2004; Ngo-Giang-Huong et al., 2001; Rouzioux et al., 2005; Viard et al., 2004; Vitone et al., 2005), only a few have reported the level of integrated DNA (Carr et al., 2007; Chun et al., 1997a; Chun et al., 1995; Chun et al., 1997b; Ibanez et al., 1999; Izopet et al., 2002; Koelsch et al., 2008; Ostrowski et al., 1999).

Currently there are three PCR assays that measure HIV integration: linker ligation (Vandegraaff et al., 2001), inverse PCR (Chun et al., 1997a), and *Alu*-PCR (Brussel, Delelis, and Sonigo, 2005; Brussel and Sonigo, 2003; Butler, Hansen, and Bushman, 2001; O'Doherty et al., 2002). Both endpoint and kinetic PCR methods have been applied to these assays, and both methods have their advantages: endpoint PCR is usually more sensitive and kinetic PCR provides superior quantitation. Studies using endpoint PCR integration assays (Chun et al., 1997a; Chun et al., 1998; Chun et al., 1995; Chun et al., 1997b; Ostrowski et al., 1999) revealed the groundbreaking finding that resting CD4+ T cells contain integrated DNA and contribute to viral reservoirs (Chun et al., 1997a; Chun et al., 1995). However, the major limitations of end point PCR are that it is too labor intensive for the high throughput needed for clinical samples, and it provides poor quantitation. For example, two studies using endpoint PCR assays to compare integration levels in total PBMCs from patients on and off highly active anti-retroviral therapy (HAART) reported conflicting results (Ibanez et al., 1999; Izopet et al., 2002). The conflicting results were in part related to the wide uncertainty in early estimates of HIV integration because the variation caused by sampling rare events was not addressed. An additional source of error in the measurements may have come from false positives; unintegrated DNA may have contributed to the signal.

Many kinetic PCR integration assays have been developed, and kinetic PCR can control for false positive signals better than endpoint PCR, as we described by including *gag*-only controls (Agosto et al., 2007; O'Doherty et al., 2002). However, none of the kinetic PCR assays that have been developed are sensitive enough to measure integration in patient samples. For example, a recent study proposed a kinetic PCR integration assay for clinical use, but the assay did not detect integration in ~50% of patient PBMCs (Carr et al., 2007). Thus, integration data was only obtained for half the patients.

Here, we report a kinetic PCR assay, derived from our original two-step kinetic *Alu*-PCR integration assay (O'Doherty et al., 2002), that is sensitive enough to measure HIV integration precisely in PBMC samples from patients. To do this, we redesigned our primers and probes to match more conserved regions of the HIV genome and we incorporated a technique that repetitively samples DNA (Agosto et al., 2007). However, even with incorporation of the

repetitive sampling technique to patient samples, the assay still lacked the required sensitivity (unpublished observations). Here we show that we can further increase the sensitivity of our integration assay by increasing the number of cycles in the 1st PCR reaction. Previously, we limited the number of cycles to maintain a large dynamic range (i.e. to ensure that substrates are not limiting). However, in patient samples the proviral levels are low and dynamic range is small. Under these conditions, a dramatic increase in sensitivity can be obtained by increasing cycle number without compromising quantitation. We used this new kinetic *Alu*-PCR integration assay to measure proviral levels in PBMCs from patients on and off HAART. Compared to patients not on HAART, we found that patients on HAART had significantly lower levels of integrated HIV DNA ($p=0.007$). Furthermore, we found the level of integrated DNA was higher than the original estimates in patients off HAART (Ibanez et al., 1999; Izopet et al., 2002; Koelsch et al., 2008).

Results

Increasing PCR cycle number increases integration assay sensitivity (Table 1)

Previously we showed that the sensitivity of our standard integration assay could be enhanced ~40-fold by repetitive sampling (Agosto et al., 2007), but when applied to patient samples, it was still not sufficiently sensitive to measure integration. Although we had previously optimized our standard integration assay for cycle number, extension time, and enzyme concentration (O'Doherty et al., 2002; Swiggard et al., 2005), now we set out to increase the sensitivity of our repetitive sampling-based assay to detect low integration levels.

To determine the optimal PCR conditions at low proviral numbers we first created a low copy number sample by diluting the integration standard (IS) (Agosto et al., 2007) to 20 proviruses in 15,000 uninfected genomes. We then assayed the diluted standard repetitively while varying cycle number, enzyme concentration, and extension time. For each condition, we measured the average *Alu*-*gag* cycle threshold, the average *gag*-only cycle threshold, and calculated the difference between these values (Table 1). The optimal conditions were defined as those that gave the greatest difference between the *Alu*-*gag* and *gag*-only signals.

We found that, by increasing the number of cycles in the first PCR reaction from 20 to 40, we increased the difference between the *Alu*-*gag* and the *gag*-only signal to a level that was most statistically significant. Under these new conditions, substrates were not limiting because a dose-response was preserved when we performed serial 2-fold dilutions of proviruses from 1,000 to 62.5 proviruses (not shown). Consistent with our prior work, the dose-response was lost at higher concentrations of provirus (between 1,000 and 100,000) when 40 cycles of amplification were used (not shown). We further optimized amplification conditions by doubling the amount of enzyme and by increasing the extension time from 2.5 to 3.5 minutes; however, the effect of these two modifications on increasing the difference between *Alu*-*gag* and *gag*-only signals was small relative to the effect of increasing the cycle number (not shown).

Redesign of the primer-probe pair to a conserved region of the HIV genome to increase the number of patient sequences detected (Figure 1)

In order to better match the sequences in the Los Alamos National Laboratory (LANL) database (Leitner et al., 2005), we redesigned the primers and probes used in our original assay. To do this, we surveyed the LANL database for the most conserved regions of the HIV genome. We slightly modified the original forward and reverse primers by shifting their positions relative to the LANL database by 3 and 6 nucleotides, respectively, compared to our original pair (Agosto et al., 2007). This change resulted in primers that bound to more highly conserved

regions in the HIV genome: the last 3 and 4 nucleotides of each primer are perfect matches with the database; the remaining nucleotides are 98–100% conserved (Figure 1).

Although we were unable to identify a region for the probe that was as highly conserved, we prepared a wild-type probe that has been previously described (Yun, Fredriksson, and Sonnerborg, 2002) and two degenerate probes that were perfect matches for the two most frequent mutations which occurr 9% and 4% of the time (Figure 1). We analyzed between 427 and 627 sequences to determine the frequency of mutations in the primers and probes. None of the mutations that are shown are linked. These three probes were mixed in equal concentrations for the kinetic PCR reaction. When we tested the new primer-probe set and compared it to the original primer-probe set, we found that both showed near 100% amplification efficiency, calculated as described (Applied Biosystems, 2004). In other words, both sets of primers amplify efficiently, but the new set is a better match to patient sequences and so will pick up more sequences.

Generation of a standard curve using our integration standard (Figure 2)

To mimic the low integration frequencies in patient samples and to determine the sensitivity of our integration assay, we calculated the proviral number in the IS cells and diluted the IS cells in uninfected PBMCs as described (Agosto et al., 2007). We calculated the proviral number in the IS cell line using routine quantitative DNA PCR because all the HIV DNA in the IS is integrated (Agosto et al., 2007). We performed *Alu-gag* amplification on IS samples in 40 replicates at multiple proviral concentrations (Figure 2A). We consistently assayed 1.5×10^4 cells per reaction (IS cells + uninfected PBMCs) to maintain a constant number of *Alu* sites. We kept the number of *Alu* sites constant because we previously determined that the number of *Alu* sites per reaction affects the efficiency of PCR amplification.

We previously showed that our IS contains diverse integration sites (Agosto et al., 2007; O'Doherty et al., 2002); and because our IS accurately models integration *in vivo*, some integration events are detectable and some are not (Agosto et al., 2007; O'Doherty et al., 2002). We found that when 160 proviruses per reaction were assayed repetitively, the *Alu-gag* signals did not overlap with the background *gag*-only signals (Figure 2A; *gag*-only curves are not shown, but brackets denote their location). When 40 proviruses per reaction were assayed repetitively, although a few *Alu-gag* signals overlapped the *gag*-only signal, the majority of *Alu-gag* signals did not (Figure 2A). As the number of proviruses per reaction decreased, the fraction of the samples that gave a positive signal decreased (Figure 2A).

We determined there was a linear relationship between the logarithim of the cycle threshold and the logarithm of the proviral number. For the integration standard, we calculated the natural log of the cycle threshold (ln*Ct*) and plotted the average of the ln*Ct* against the natural log of the proviral number (ln*n*). We observed a linear relationship between ln*n* and ln*Ct* Figure 2B This linear relationship is represented by the equation $\ln n = D\ln Ct + E$ (Figure 2B), where *n* represents proviral number, *Ct* represents cycle threshold response, D= −8.2619, E= 29.56, and R^2= 0.975. Having derived a standard equation, we could apply it to the results of *Alu-gag* PCR on patient samples, and calculate the proviral number in these samples.

Our new integration assay is sufficiently sensitive to detect integration in patient samples (Figure 3, Table 2)

We wanted to test whether our improved assay was sensitive enough to measure integration in patient PBMCs. To do this, we purified DNA from PBMCs of 10 patients on HAART and 6 patients off HAART, then performed our new two-step PCR integration assay on 40 samples for each patient repetitively. We obtained a distribution of *Alu-gag* amplification curves for each patient (Figure 3, representative curves). To measure integration levels in patients, we

first determined if integration was detectable by performing a one-tailed t-test to make sure that our *Alu-gag* was significantly lower than *gag*-only. Then, we compared their *Alu-gag* signals to the *Alu-gag* signals generated by our diluted IS samples. We determined the proviral number for each patient by obtaining the cycle threshold (*Ct*) for each *Alu-gag* amplification curve, taking the natural log of the cycle threshold (ln*(Ct)*). Next, we calculated the average ln (Ct) for each patient and inserted the average ln*(Ct)* into the equation ln$n = D*average(\ln Ct) + E$, where D= −8.26, E= 29.56. Lastly, we calculated the proviral number by taking the exponential of ln(*n*) and calculated the 95% confidence intervals, which are asymmetric because of the logarithmic transformation. We found that our improved assay was sensitive enough to detect proviral loads as low as 0.5 integration events in 10,000 PBMCs (Table 2, patients 1, 6, 7, and 8). The average *Alu-gag* and *gag*-only signals are provided (Supplemental Table) and demonstrate that the *Alu-gag* signal was always significantly lower than the *gag*-only signal by a one-tailed Student's t-test.

Unintegrated patient DNA does not contribute significantly to the integration assay signal (Figure 4, Table 3)

DNA extracted from patient PBMCs contains a mixture of HIV DNA that is integrated into the host chromosome, and HIV DNA that is unintegrated and present as linear or circular forms. We considered the possibility that unintegrated HIV DNA may contribute to the *Alu-gag* integration assay signal. If this were the case, then our measurements of integrated HIV DNA would be higher than the actual number of proviruses.

To determine whether unintegrated DNA contributes to the *Alu-gag* signal attributed to integrated DNA, we prepared DNA from patient PBMCs, separated the chromosomal, linear, and circular fractions by agarose gel electrophoresis, extracted DNA from the gel, and performed *Alu-gag* PCR on individual fractions as well as on a mixture. When we assayed chromosomal DNA samples, the integration signal was stronger than the background signal: on average the *Alu-gag* curves crossed the cycle threshold (Ct) at lower cycle numbers than the background *gag*-only curves (Fig 4, panel A; Table 4, row 1). By comparison, when we assayed linear and circular DNA samples, the integration signal equaled the background signal: *Alu-gag* and *gag*-only curves crossed the Ct at the same cycle number (Figure 4, panels B and C; Table , rows 2 and 3). Therefore, HIV integration was detected only in chromosomal DNA samples. Finally, we found that the *Alu-gag* signal from a mixture of the three fractions, was comparable to that from the chromosomal fraction alone (Figure 4, compare panel D to A; Table 3, compare bolded values). Therefore, we conclude that, in a patient sample containing a mixture of integrated and unintegrated HIV DNA, unintegrated DNA does not contribute significantly to the *Alu-gag* signal.

Unintegrated DNA contributes minimally to the integration signal (Table 4)

In a second approach to determine whether unintegrated HIV DNA contributes to the *Alu-gag* signal from integrated DNA, we modeled the ratio of unintegrated-to-integrated DNA in patient samples and measured integration. We added 100-fold excess of unintegrated HIV plasmid DNA (U), NG38, to our integration standard (IS) DNA, because a 100:1 ratio of unintegrated-to-integrated DNA was close to the highest ratio that we detected in patient samples. We found that when we performed *Alu-gag* and *gag*-only PCR on 800 copies of unintegrated DNA (800 U), the *Alu-gag* and *gag*-only signals were equivalent indicating that the sample was negative for integration (Table 4). When 8 copies of integrated DNA (8 IS) were assayed, the *Alu-gag* signal was stronger (detected at a lower cycle number) than the *gag*-only signal, indicating that integration was detected (Table 4). When we added 100-fold excess of unintegrated DNA to integrated DNA (800 U + 8 IS), the *Alu-gag* signal remained stronger than the *gag*-only signal (Table 4). The *Alu-gag* signal from 800 U + 8 IS was slightly stronger than that from 8 IS (Table 4). This slightly stronger signal translated into only a 2-

fold difference when we calculated the number of proviruses per well: 7 proviruses/well in the 8 IS sample, 15 proviruses/well in the 800 U+ 8 IS sample (Table 2). Therefore, we concluded that unintegrated DNA contributes minimally to the integration assay signal.

Patients on HAART have lower levels of integrated HIV DNA in PBMCs (Figure 5, Table 2)

We hypothesized that patients on HAART have lower levels of integrated DNA than patients not on HAART. To test this hypothesis, we measured integration levels in patients on HAART and off HAART, averaged the integration level in each group, and performed a Wilcoxon signed-rank test (Figure 5, $p= 0.007$). We found that there was a difference between the proviral levels in the two groups: patients on HAART had lower levels of integration than patients off HAART (Figure 5).

All the patients off HAART had a viral load >1000, except for patient 11 with an unknown viral load (Table 5). All the patients on HAART had an undetectable viral load the day of donation (Table 5) except patients 4 and 5 who had barely detectable viral loads. Both populations had relatively preserved CD4 counts (≥290 cells/μl) (Table 5). Prior studies suggest that HAART treatment results in modestly lower concentrations of viral DNA (Ngo-Giang-Huong et al., 2001;Viard et al., 2004). We wanted to measure the amount of total DNA in our patient samples. Using the primer probe set shown in Figure 1, but omitting *Alu-gag* pre-amplification, we measured the level of total HIV DNA. Consistent with prior literature, there is a significant difference in the level of total DNA between the patients on and off HAART (Table 5) as assessed by the Wilcoxon signed-rank test, $p= 0.02$. We also calculated the ratio of total DNA to integrated DNA in the two patient groups. We found that HAART affected the level of integrated DNA to a greater extent than the level of unintegrated DNA (Table 2 and Table 5); however, larger numbers of samples need to be examined before additional conclusions can be made about the ratio of integrated to unintegrated DNA.

Discussion

Here we describe a new integration assay that is a significant advance over prior technology. Our improved kinetic PCR assay is sufficiently sensitive to measure HIV integration and provide error estimates in PBMC samples from infected individuals (Table 2). Furthermore, results obtained with the assay suggest that the level of integrated DNA is lower in patients on effective HAART than in patients not on HAART. Although this result may seem obvious, two prior reports failed to detect this difference (Carr et al., 2007;Ibanez et al., 1999). Our ability to detect this difference suggests our assay may be more precise than prior assays. Nonetheless, longitudinal studies following the level of integration over time after HAART is initiated will be required to determine the effect of HAART.

Our new integration assay overcomes the disadvantages of endpoint PCR, as well as the low sensitivity of prior kinetic PCR techniques, by incorporating repetitive sampling and optimizing conditions for rare event detection. Repetitive sampling increased the sensitivity of the assay, permitted calculation of proviral numbers and permitted calculation of confidence intervals. Notably, prior assays did not provide calculations of confidence intervals. We further optimized the assay by recognizing that we could sacrifice the range of detection of integration to enhance sensitivity by increasing the number of PCR cycles.

Prior to the development of our new assay, studies using endpoint PCR assays to measure HIV integration in patient samples reported several important findings (Chun et al., 1997a; Chun et al., 1998; Chun et al., 1995; Chun et al., 1997b; Ostrowski et al., 1999) such as the level of integration, the concentration of proviruses in memory cells, and the failure of HAART to lower the level of integrated HIV DNA in resting CD4+ T cells. However, endpoint PCR has

several disadvantages: it is semi-quantitative, labor-intensive, and does not permit calculation of confidence intervals.

Our new assay can be used to expand upon the findings obtained with endpoint PCR. Specifically, it can be used to refine the initial estimates of the level of integrated DNA in several CD4+ subsets. Since our assay is more sensitive, it should also provide proviral numbers in cell subsets where integration was previously undetectable. In addition, because our assay has tighter confidence intervals, it can be used to follow small fluctuations in integration and so may be useful in determining if HAART treatment leads to clearance of integrated DNA from subsets of CD4+ cells.

To our knowledge, our integration assay is the most sensitive assay currently available and the only assay that provides calculation of confidence intervals. Our measurements may also be more accurate because we used a polyclonal integration standard. This standard more closely models *in vivo* integration and was used to generate the standard curve used to calculate proviral number in patient samples. Nonetheless, we may be able to refine our assay to make it more accurate and more sensitive. For example, we are developing mathematical models that will correct for the small signal that unintegrated DNA contributes; although at most, the contribution from unintegrated DNA results in a 2-fold overestimate in the number of proviruses and only in a subset of patient samples with strong *gag*-only signals. This correction is not likely required in our patients on HAART because these patients show very little *gag*-only priming (Supplemental Table), i.e. the signal from total DNA and *gag*-only priming is similar. We speculate that little *gag*-only priming occurs in some patients with relatively high levels of unintegrated DNA (such as patients 2 and 7 on HAART) because the unintegrated DNA may be discontinuous. This correction may be relevant for 3 of the patients off HAART (such as patients 11, 12, and 14) since there was significant *gag*-only priming in these 3 patients (Supplemental Table). This is the first report that we are aware of that quantitates the contribution from unintegrated DNA.

Application of our assay to larger numbers of patient samples may address important issues in HIV pathogenesis. Even if the majority of integrated proviruses are defective (Coffin, 1995; Han et al., 2007; Lassen et al., 2004; Lehrman et al., 2005), our finding that patients on HAART have lower integration levels suggests that some populations of mononuclear cells bearing proviruses can be cleared of provirus with therapy and so should be monitored. In addition, with more precise measurements of HIV integration, it is possible to test whether the level of integrated DNA correlates with disease progression as has been shown for viral RNA load (Mellors et al., 1995). It has been shown, using kinetic PCR, that the level of total viral DNA within PBMCs also correlates weakly with disease progression (Kostrikis et al., 2002; Ngo-Giang-Huong et al., 2001; Rouzioux et al., 2005; Viard et al., 2004). With this assay, we could also measure the rate of decline of integrated DNA in total PBMCs and even within cellular subsets after a patient begins HAART to assess the effect of therapy longitudinally.

It remains unclear why only a small fraction of CD4+ resting T cells bearing integrated HIV DNA are latently infected, i.e. capable of producing infectious HIV when stimulated (Coffin, 1995; Han et al., 2007; Lassen et al., 2004). Possible explanations are that many of these cells bear proviruses that are either not transcribed, or do not produce infectious virions when stimulated. Rigorous quantitation of the level of integrated DNA, the frequency of cells capable of transcribing HIV proviruses (Haase, 2005), and the frequency of cells capable of producing infectious virions (Han et al., 2007; Lassen et al., 2004) may give us a better understanding of latency. In addition, with the advent of additional anti-HIV therapies, such as fusion inhibitors and integrase inhibitors, it is now possible to treat patients with intensified therapies. A sensitive assay for monitoring integration levels may be an important tool for monitoring and

quantitating the additional benefits of intensified therapy when viral load is already undetectable.

Methods

Cell lines, plasmids, and viruses

The CD4+ T-lymphoblastoid cell line CEM-ss (Foley et al., 1965; Nara and Fischinger, 1988) was maintained at 1–5 × 10^5 cells per ml. The culture medium was RPMI 1640 supplemented with 10% heat-inactivated fetal bovine serum, 25 mM HEPES, with 100μg/ml penicillin-streptomycin (Invitrogen Life Technologies). Virions pseudotyped with vesicular stomatitis virus protein G (VSV-G) (Blumenthal et al., 1987; Emi, Friedmann, and Yee, 1991) were collected 24 hours after transfection of 293T cells with pVSV-G (pHIT) (Fouchier et al., 1997) and pNL4-3Δenv/GFP/Hyg^R. The reporter virus was derived from pNL4-3, an X4-tropic HIV clone (Adachi et al., 1986). The *nef* open reading frame (ORF) was replaced with a green fluorescent protein (GFP) and hygromycin resistance cassette which contained an internal ribosome entry site between the two ORFs. The plasmid (pNG38) was prepared by removing the human genomic sequence form HXB-2 (personal communications with Nathan Gaddis).

Preparation of the Integration Standard (IS) cell line

The integration standard cell line (IS) was prepared as described (Agosto et al., 2007). The standard contains diverse integration sites with some integration sites close to an *Alu* repeat and others far away. We estimated that about 10% of proviruses are detectable by our methods at low proviral copy numbers (Figure 2A).

Patients' blood samples

Patients on and off HAART therapy (both for at least three months) were recruited using an IRB approved protocol to donate blood. Patients 12 and 13 were never on HAART. Patients 11, 14, 15, and 16 were on HAART for 3months, 9, 4 and 7 years, respectively. Patients on HAART had ≤400 copies of viral RNA/ml. PBMCs were prepared from anticoagulated blood by Ficoll-Hypaque separation (Swiggard et al., 2004). Total DNA was prepared (Blood and Cell Culture DNA Maxi Kit, QIAGEN).

PCR conditions

Two step PCR amplification was performed as described (Agosto et al., 2007; O'Doherty et al., 2002) with some modifications. Briefly, the first amplification was performed on dilutions of the IS cells as well as patient samples and no template controls. The sequence of the first step amplification primers were: genomic *Alu* forward 5' GCC TCC CAA ACT GCT GGG ATT ACA G-3' and HIV *gag* reverse 5' GTT CCT GCT ATG TCA CTT CC-3'. The *gag* primer is different from the previously described primer (O'Doherty et al., 2002). It provides a better consensus sequence than the original primer and provides more efficient *Alu*-*gag* amplification. The IS was diluted in uninfected PBMC DNA to keep the number of *Alu* sites per reaction constant. The reactions were conducted in 50μl: 10 mM Tris-HCl, pH 8.0; 1.8 mM $MgCl_2$; 1mM mixed dNTPs; 100 nM *Alu* forward primer; 600 nM *gag* reverse primer; and 0.05 units of Platinum Taq DNA polymerase/μl (Invitrogen Life Technologies). The thermal cycler (DNA Engine PTC-200, MJResearch) was programmed to perform a two-minute hot start at 95°C, followed by 40 cycles of the following: denaturation at 95°C for 15s, annealing at 50°C for 15s and extension at 72°C for 3 min 30 sec. Linear, one strand amplification (priming) was also monitored by performing the first amplification PCR with the *gag* primer alone.

The second round real-time quantitative PCR was performed using 10 μl of the material from the first amplification. These were run with an HIV-1 copy number standard (ACH-2) (Folks et al., 1989). The sequences of the primers were: LTR (R) forward, 5'-TTA AGC CTC AAT AAA GCT TGC C-3'; LTR (U5) reverse, 5'-GTT CGG GCG CCA CTG CTA GA-3'. The LTR Taqman probes were labeled at their 5' terminus with the reporter fluorophore 6-carboxyfluorescein (FAM) and at their 3' terminus with the quencher tetramethylrhodamine (TAMRA). The wild type probe had the following sequence: 5'-FAM-CCA GAG TCA CAC AAC AGA GGG GCA CA-TAMRA-3' as described (Yun, Fredriksson, and Sonnerborg, 2002). The two degenerate probes had the sequences listed in Figure 1. Reactions were carried out in a volume of 20μl containing: 10 mM Tris-HCl, pH 8.0; 75 mM KCl; 5.5 mM $MgCl_2$; 500 nM carboxy-X-rhodamine (ROX, Molecular Probes) as a passive reference; 1.2 mM freshly added dNTPs; 250 nM LTR forward and reverse primers; 100 nM each Taqman probe; and 0.05 units of Platinum Taq DNA polymerase/μl. The reactions were performed on an ABI7500 instrument running 7500 Fast System SDS software with the following thermal program: 20 sec hot start at 95°C, followed by 40 cycles of: denaturation at 95°C for 3 sec, annealing and extending at 60°C for 30 sec. One step reactions were performed to measure the total HIV (RU5) DNA by simply eliminating the first *Alu-gag* amplification step.

We constructed two degenerate probes, because two mutations were relatively common. We found no difference in amplification efficiency of HIV integrated DNA in the presence or absence of the degenerate probes (not shown).

The quantity of DNA was determined by $OD_{260/280}$. The number of genomes was calculated given that ~3.18×10^9 bp are present per genome. These numbers were used to calculate the level of total and integrated HIV DNA per cell.

Repetitive sampling to measure integration at low proviral copy number

Alu-gag PCR and *gag*-only PCR were performed repetitively on 10 μl aliquots of DNA at 2 μg/ml from the IS line and from patient samples. Then HIV-1 specific kinetic PCR was performed on 10μl aliquots of the first reaction. After the kinetic PCR reaction, the cycle thresholds (Ct) for each well were determined, i.e. the cycle value where the accumulating fluorescence (from fluorescently labeled amplicons) crossed a specified fluorescent threshold value. In all of the experiments described here, the fluorescent threshold value was set at 0.01 for data analysis. As previously shown (Agosto et al., 2007), the average natural log of the cycle thresholds are linearly related to the natural log of the proviral number. The standard equation was generated by finding the linear regression of the average natural log of the cycle threshold values from each concentration of IS and the natural log of the proviral number. The proviral number for patient samples was then calculated using this standard curve. To do this, the natural logarithm of each cycle threshold was obtained and averaged and standard errors were calculated. These values (average ln(Ct) +/− std error ln(Ct) were entered into the equation described in Figure 2b. Because of the logarithmic transformation to our data, the errors are asymmetrical for proviral numbers.

Supplementary Material

Refer to Web version on PubMed Central for supplementary material.

Acknowledgments

This study was supported in part by NIH grants R01 AI058862-01 (U.O.) and R21 AI064031 (U.O.). We would like to thank Liz Colston, Luis Agosto, Drew Weissman, and Rick Bushman for critical reading of this manuscript. We are grateful to Penn CFAR and Farida Shaheen for excellent technical guidance regarding real time kinetic PCR. We are grateful to Joseph Quinn and Debbie Gudonis for recruiting patients for blood donation and to the ACTG program at Penn, directed by Ian Frank.

References

Adachi A, Gendelman HE, Koenig S, Folks T, Willey R, Rabson A, Martin MA. Production of acquired immunodeficiency syndrome-associated retrovirus in human and nonhuman cells transfected with an infectious molecular clone. J Virol 1986;59(2):284–291. [PubMed: 3016298]

Agosto LM, Yu JJ, Dai J, Kaletsky R, Monie D, O'Doherty U. HIV-1 integrates into resting CD4+ T cells even at low inoculums as demonstrated with an improved assay for HIV-1 integration. Virology 2007;368(1):60–72. [PubMed: 17631931]

Applied Biosystems. Guide to Performing Relative Quantitation of Gene Expression Using Real-Time Quantitative PCR. 2004. p.
12
http://www3.appliedbiosystems.com/cms/groups/mcb_marketing/documents/generaldocuments/cms_042380.pdf

Blumenthal R, Bali-Puri A, Walter A, Covell D, Eidelman O. pH-dependent fusion of vesicular stomatitis virus with Vero cells. Measurement by dequenching of octadecyl rhodamine fluorescence. J Biol Chem 1987;262(28):13614–13619. [PubMed: 2820977]

Brenchley JM, Hill BJ, Ambrozak DR, Price DA, Guenaga FJ, Casazza JP, Kuruppu J, Yazdani J, Migueles SA, Connors M, Roederer M, Douek DC, Koup RA. T-cell subsets that harbor human immunodeficiency virus (HIV) in vivo: implications for HIV pathogenesis. J Virol 2004;78(3):1160–1168. [PubMed: 14722271]

Brussel A, Delelis O, Sonigo P. Alu-LTR real-time nested PCR assay for quantifying integrated HIV-1 DNA. Methods Mol Biol 2005;304:139–154. [PubMed: 16061972]

Brussel A, Sonigo P. Analysis of early human immunodeficiency virus type 1 DNA synthesis by use of a new sensitive assay for quantifying integrated provirus. J Virol 2003;77(18):10119–10124. [PubMed: 12941923]

Brussel A, Sonigo P. Evidence for gene expression by unintegrated human immunodeficiency virus type 1 DNA species. J Virol 2004;78(20):11263–11271. [PubMed: 15452245]

Burgard M, Izopet J, Dumon B, Tamalet C, Descamps D, Ruffault A, Vabret A, Bargues G, Mouroux M, Pellegrin I, Ivanoff S, Guisthau O, Calvez V, Seigneurin JM, Rouzioux C. HIV RNA and HIV DNA in peripheral blood mononuclear cells are consistent markers for estimating viral load in patients undergoing long-term potent treatment. AIDS Res Hum Retroviruses 2000;16(18):1939–1947. [PubMed: 11153076]

Butler SL, Hansen MST, Bushman FD. A quantitative assay for HIV DNA integration in vivo. Nature Medicine 2001;7:631–634.

Carr JM, Cheney KM, Coolen C, Davis A, Shaw D, Ferguson W, Chang G, Higgins G, Burrell C, Li P. Development of methods for coordinate measurement of total cell-associated and integrated human immunodeficiency virus type 1 (HIV-1) DNA forms in routine clinical samples: levels are not associated with clinical parameters, but low levels of integrated HIV-1 DNA may be prognostic for continued successful therapy. J Clin Microbiol 2007;45(4):1288–1297. [PubMed: 17314225]

Chun TW, Carruth L, Finzi D, Shen X, DiGiuseppe JA, Taylor H, Hermankova M, Chadwick K, Margolick J, Quinn TC, Kuo YH, Brookmeyer R, Zeiger MA, Barditch-Crovo P, Siliciano RF. Quantification of latent tissue reservoirs and total body viral load in HIV-1 infection. Nature 1997a; 387:183–188. [PubMed: 9144289]

Chun TW, Engel D, Berrey MM, Shea T, Corey L, Fauci AS. Early establishment of a pool of latently infected, resting CD4(+) T cells during primary HIV-1 infection. Proceedings of the National Academy of Sciences USA 1998;95:8869–8873.

Chun TW, Finzi D, Margolick J, Chadwick K, Schwartz D, Siliciano RF. In vivo fate of HIV-1-infected T cells: quantitative analysis of the transition to stable latency. Nat Med 1995;1(12):1284–1290. [PubMed: 7489410]

Chun TW, Stuyver L, Mizell SB, Ehler LA, Mican JA, Baseler M, Lloyd AL, Nowak MA, Fauci AS. Presence of an inducible HIV-1 latent reservoir during highly active antiretroviral therapy. Proceedings of the National Academy of Sciences USA 1997b;94:13193–13197.

Coffin JM. HIV population dynamics in vivo: implications for genetic variation, pathogenesis, and therapy. Science 1995;267:483–489. [PubMed: 7824947]

Debiaggi M, Zara F, Pistorio A, Bruno R, Sacchi P, Patruno SF, Achilli G, Romero E, Filice G. Quantification of HIV-1 proviral DNA in patients with undetectable plasma viremia over long-term highly active antiretroviral therapy. Int J Infect Dis 2000;4(4):187–193. [PubMed: 11231180]

Douek DC, Brenchley JM, Betts MR, Ambrozak DR, Hill BJ, Okamoto Y, Casazza JP, Kuruppu J, Kunstman K, Wolinsky S, Grossman Z, Dybul M, Oxenius A, Price DA, Connors M, Koup RA. HIV preferentially infects HIV-specific CD4+ T Cells. Nature 2002 May;417:95–98. [PubMed: 11986671]

Emi N, Friedmann T, Yee JK. Pseudotype formation of murine leukemia virus with the G protein of vesicular stomatitis virus. J Virol 1991;65(3):1202–1207. [PubMed: 1847450]

Foley GE, Lazarus H, Farber S, Uszman BG, Boone BA, McCarthy RE. Continuous culture of human lymphoblasts from peripheral blood of a child with acute leukemia. Cancer 1965;18(4):522–529. [PubMed: 14278051]

Folks TM, Clouse KA, Justement J, Rabson A, Duh E, Kehrl JH, Fauci AS. Tumor necrosis factor alpha induces expression of human immunodeficiency virus in a chronically infected T-cell clone. Proc Natl Acad Sci U S A 1989;86(7):2365–2368. [PubMed: 2784570]

Fouchier RAM, Meyer BE, Simon JHM, Fischer U, Malim MH. HIV-1 infection of non-dividing cells: evidence that the amino-terminal basic region of the viral matrix protein is important for Gag processing but not for post-entry nuclear import. European Molecular Biology Organization Journal 1997;16:4531–4539.

Gibellini D, Vitone F, Schiavone P, Ponti C, La Placa M, Re MC. Quantitative detection of human immunodeficiency virus type 1 (HIV-1) proviral DNA in peripheral blood mononuclear cells by SYBR green real-time PCR technique. J Clin Virol 2004;29(4):282–289. [PubMed: 15018857]

Haase AT. Perils at mucosal front lines for HIV and SIV and their hosts. Nat Rev Immunol 2005;5(10): 783–792. [PubMed: 16200081]

Han Y, Wind-Rotolo M, Yang HC, Siliciano JD, Siliciano RF. Experimental approaches to the study of HIV-1 latency. Nat Rev Microbiol 2007;5(2):95–106. [PubMed: 17224919]

Ibanez A, Puig T, Elias J, Clotet B, Ruiz L, Martinez MA. Quantification of integrated and total HIV-1 DNA after long-term highly active antiretroviral therapy in HIV-1-infected patients. Aids 1999;13 (9):1045–1049. [PubMed: 10397534]

Izopet J, Cazabat M, Pasquier C, Sandres-Saune K, Bonnet E, Marchou B, Massip P, Puel J. Evolution of total and integrated HIV-1 DNA and change in DNA sequences in patients with sustained plasma virus suppression. Virology 2002;302(2):393–404. [PubMed: 12441083]

Jubault V, Burgard M, Le Corfec E, Costagliola D, Rouzioux C, Viard JP. High rebound of plasma and cellular HIV load after discontinuation of triple combination therapy. Aids 1998;12(17):2358–2359. [PubMed: 9863885]

Kabamba-Mukadi B, Henrivaux P, Ruelle J, Delferriere N, Bodeus M, Goubau P. Human immunodeficiency virus type 1 (HIV-1) proviral DNA load in purified CD4+ cells by LightCycler real-time PCR. BMC Infect Dis 2005;5(1):15. [PubMed: 15780144]

Koelsch KK, Liu L, Haubrich R, May S, Havlir D, Gunthard HF, Ignacio CC, Campos-Soto P, Little SJ, Shafer R, Robbins GK, D'Aquila RT, Kawano Y, Young K, Dao P, Spina CA, Richman DD, Wong JK. Dynamics of total, linear nonintegrated, and integrated HIV-1 DNA in vivo and in vitro. J Infect Dis 2008;197(3):411–419. [PubMed: 18248304]

Kostrikis LG, Touloumi G, Karanicolas R, Pantazis N, Anastassopoulou C, Karafoulidou A, Goedert JJ, Hatzakis A. Quantitation of human immunodeficiency virus type 1 DNA forms with the second template switch in peripheral blood cells predicts disease progression independently of plasma RNA load. J Virol 2002;76(20):10099–10108. [PubMed: 12239284]

Lassen K, Han Y, Zhou Y, Siliciano J, Siliciano RF. The multifactorial nature of HIV-1 latency. Trends Mol Med 2004;10(11):525–531. [PubMed: 15519278]

Lehrman G, Hogue IB, Palmer S, Jennings C, Spina CA, Wiegand A, Landay AL, Coombs RW, Richman DD, Mellors JW, Coffin JM, Bosch RJ, Margolis DM. Depletion of latent HIV-1 infection in vivo: a proof-of-concept study. Lancet 2005;366(9485):549–555. [PubMed: 16099290]

Leitner, TFB.; Hahn, B.; Marx, P.; McCutchan, F.; Mellors, J.; Wolinsky, S.; Korber, B. Los Alamos National Laboratories, HIV Sequence Compendium. Published by Theoretical Biology and Biophysics Group; 2005. http://www.hiv.lanl.gov/

Lillo FB, Grasso MA, Lodini S, Bellotti MG, Colucci G. Few modifications of the Cobas Amplicor HIV Monitor 1.5 test allow reliable quantitation of HIV-1 proviral load in peripheral blood mononuclear cells. J Virol Methods 2004;120(2):201–205. [PubMed: 15288963]

Mellors JW, Kinsley LA, Rinaldo CRJ, et al. Quantitation of HIV-1 RNA in plasma predicts outcome after seroconversion. Annals of Internal Medicine 1995;122:573–579. [PubMed: 7887550]

Nakajima N, Lu R, Engelman A. Human immunodeficiency virus type 1 replication in the absence of integrase-mediated dna recombination: definition of permissive and nonpermissive T-cell lines. J Virol 2001;75(17):7944–7955. [PubMed: 11483739]

Nara PL, Fischinger PJ. Quantitative infectivity assay for HIV-1 and -2. Nature 1988;332:469–470. [PubMed: 3281026]

Ngo-Giang-Huong N, Deveau C, Da Silva I, Pellegrin I, Venet A, Harzic M, Sinet M, Delfraissy JF, Meyer L, Goujard C, Rouzioux C. Proviral HIV-1 DNA in subjects followed since primary HIV-1 infection who suppress plasma viral load after one year of highly active antiretroviral therapy. Aids 2001;15(6):665–673. [PubMed: 11371680]

O'Doherty U, Swiggard WJ, Jeyakumar D, McGain D, Malim MH. A sensitive, quantitative, assay for Human Immunodeficiency Virus type 1 integration. Journal of Virology 2002;76(21):10,942–10,950.

Ostrowski MA, Chun T-W, Justement SJ, Motola I, Spinelli MA, Adelsberger J, Ehler LA, Mizell SB, Hallahan CW, Fauci AS. Both memory and CD45RA(+)/CD62L(+) naive CD4(+) T cells are infected in human immunodeficiency type 1-infected individuals. Journal of Virology 1999;73:6430–6435. [PubMed: 10400736]

Rouzioux C, Hubert JB, Burgard M, Deveau C, Goujard C, Bary M, Sereni D, Viard JP, Delfraissy JF, Meyer L. Early levels of HIV-1 DNA in peripheral blood mononuclear cells are predictive of disease progression independently of HIV-1 RNA levels and CD4+ T cell counts. J Infect Dis 2005;192(1):46–55. [PubMed: 15942893]

Swiggard WJ, Baytop C, Yu JJ, Dai J, Li C, Schretzenmair R, Theodosopoulos T, O'Doherty U. Human immunodeficiency virus type 1 can establish latent infection in resting CD4+ T cells in the absence of activating stimuli. J Virol 2005;79(22):14179–14188. [PubMed: 16254353]

Swiggard WJ, O'Doherty U, McGain D, Jeyakumar D, Malim MH. Long HIV Type 1 reverse transcripts can accumulate stably within resting CD4+ T cells while short ones are degraded. AIDS Research and Human Retroviruses 2004;20(3):285–295. [PubMed: 15117452]

Vandegraaff N, Kumar R, Burrell CJ, Li P. Kinetics of Human Immunodeficiency Virus type 1 DNA integration in acutely infected cells as determined using a novel assay for detection of integrated HIV DNA. Journal of Virology 2001;75:11253–11260. [PubMed: 11602768]

Viard JP, Burgard M, Hubert JB, Aaron L, Rabian C, Pertuiset N, Lourenco M, Rothschild C, Rouzioux C. Impact of 5 years of maximally successful highly active antiretroviral therapy on CD4 cell count and HIV-1 DNA level. Aids 2004;18(1):45–49. [PubMed: 15090828]

Vitone F, Gibellini D, Schiavone P, Re MC. Quantitative DNA proviral detection in HIV-1 patients treated with antiretroviral therapy. J Clin Virol 2005;33(3):194–200. [PubMed: 15911440]

Wu Y, Marsh JW. Selective transcription and modulation of resting T cell activity by pre-integrated HIV DNA. Science 2001;293:1503–1506. [PubMed: 11520990]

Wu Y, Marsh JW. Early transcription from nonintegrated DNA in human immunodeficiency virus infection. J Virol 2003a;77(19):10376–10382. [PubMed: 12970422]

Wu Y, Marsh JW. Gene transcription in HIV infection. Microbes Infect 2003b;5(11):1023–1027. [PubMed: 12941394]

Yun Z, Fredriksson E, Sonnerborg A. Quantification of human immunodeficiency virus type 1 proviral DNA by the TaqMan real-time PCR assay. J Clin Microbiol 2002;40(10):3883–3884. [PubMed: 12354911]

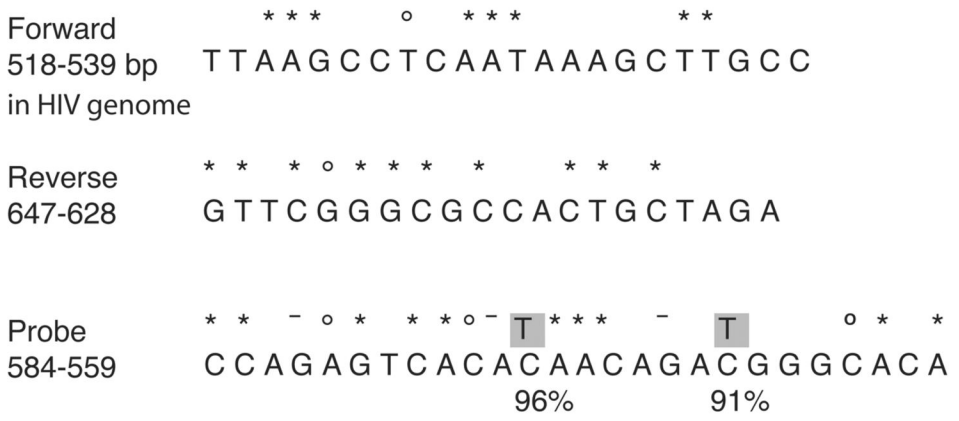

Figure 1. Sequence of the primers and probes used in the HIV integration assay

The nucleotide sequences and their positions relative to the HIV genome of the forward primer, reverse primer and probe are shown. The percent identity to the LANL HIV database consensus is indicated as follows: no symbol denotes 100% identity, an asterisk (*) above a base indicates 99% identity, a circle (○) represents 98% identity, and a dash (-) indicates 97% identity. The forward primer sits at position 518–539 in HIV genome (based on HXB-2 numbering). The reverse primer sits at bases 647–628. The fluorescent probes lie between 584–559. Two degenerate fluorescent probes were synthesized to capture the two most mutated bases, highlighted in grey. These two mutated bases are present in 9% and 4% of sequences. The primer probe sets were used to detect either total DNA (without *Alu-gag* preamplification) or to detect *Alu-gag* amplicons as described in the Methods.

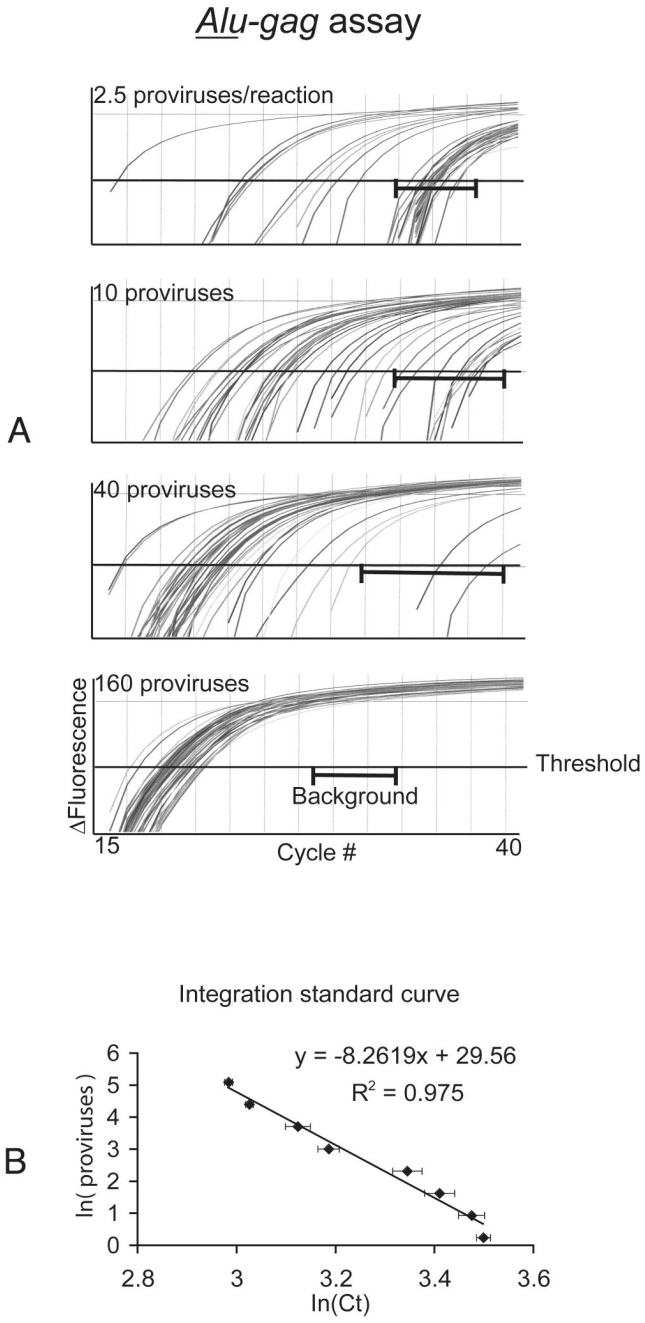

Figure 2. IS standard curve and linear regression

Alu-gag PCR was performed repetitively (N=40) on serial 4-fold dilutions of the integration standard. N represents the number of samples tested.

A. The curves generated at 2.5, 10, 40 and 160 proviruses per reaction are shown for *Alu-gag*. Background or *gag*-only signals are not shown, but the brackets (⊢⊣) represents the range of *gag*-only signals. The cycle threshold (Ct) for each sample was calculated by determining where the PCR curve crosses the horizontal line at 0.01 fluorescence units.

B. The natural log of each Ct for each curve was calculated and then averaged. A standard curve was then generated by plotting the x-axis as the average of the natural log of *Ct* and the y-axis as the natural log of the provirus quantity in the diluted standard. The provirus number

in our integration standard is known as previously described (Agosto et al., 2007). The error bars represent standard error of the mean.

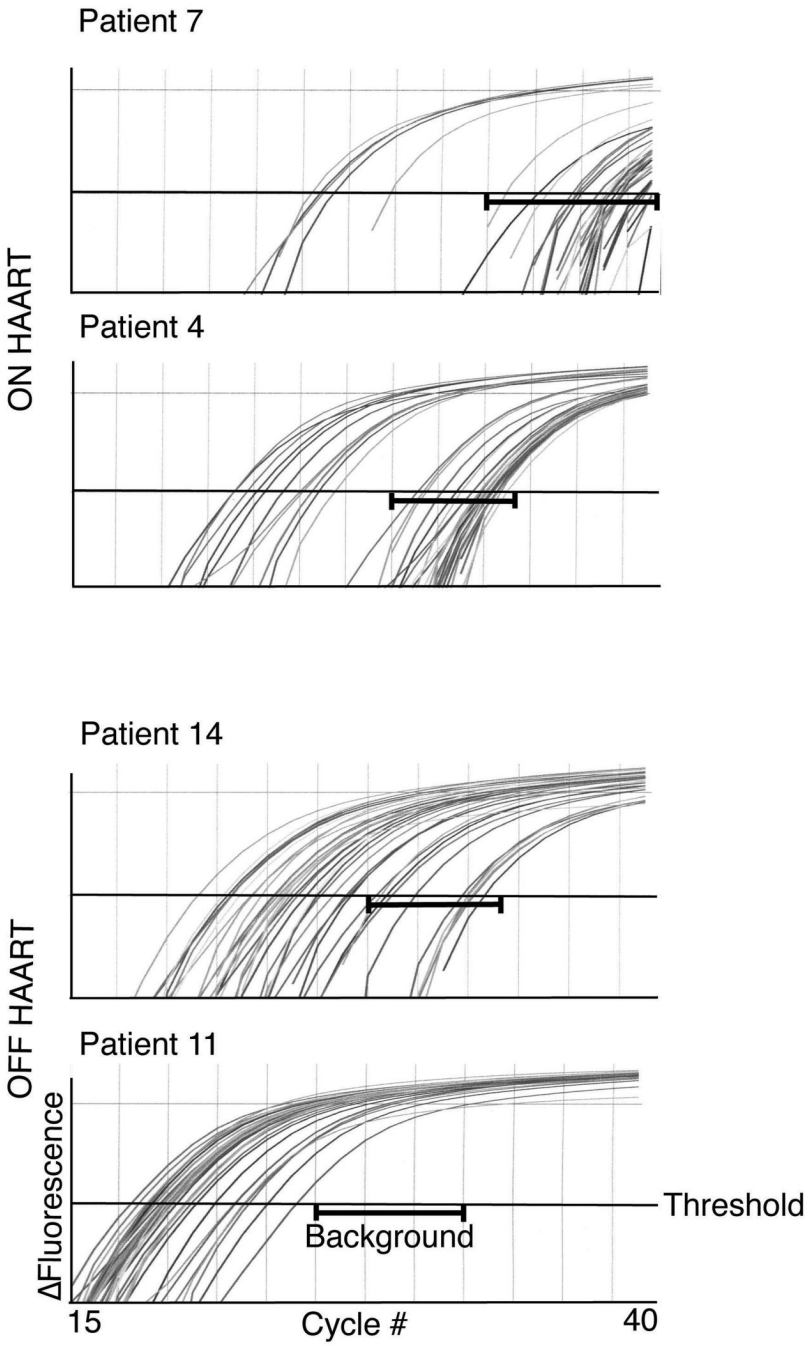

Figure 3. Representative *Alu-gag* PCR amplification curves

PBMC DNA was prepared from HIV infected individuals (Patients 4 and 7 were on HAART and Patients 11 and 14 were not on HAART). *Alu-gag* PCR was performed in 40 replicates and then HIV-1 specific kinetic PCR was performed on each replicate.

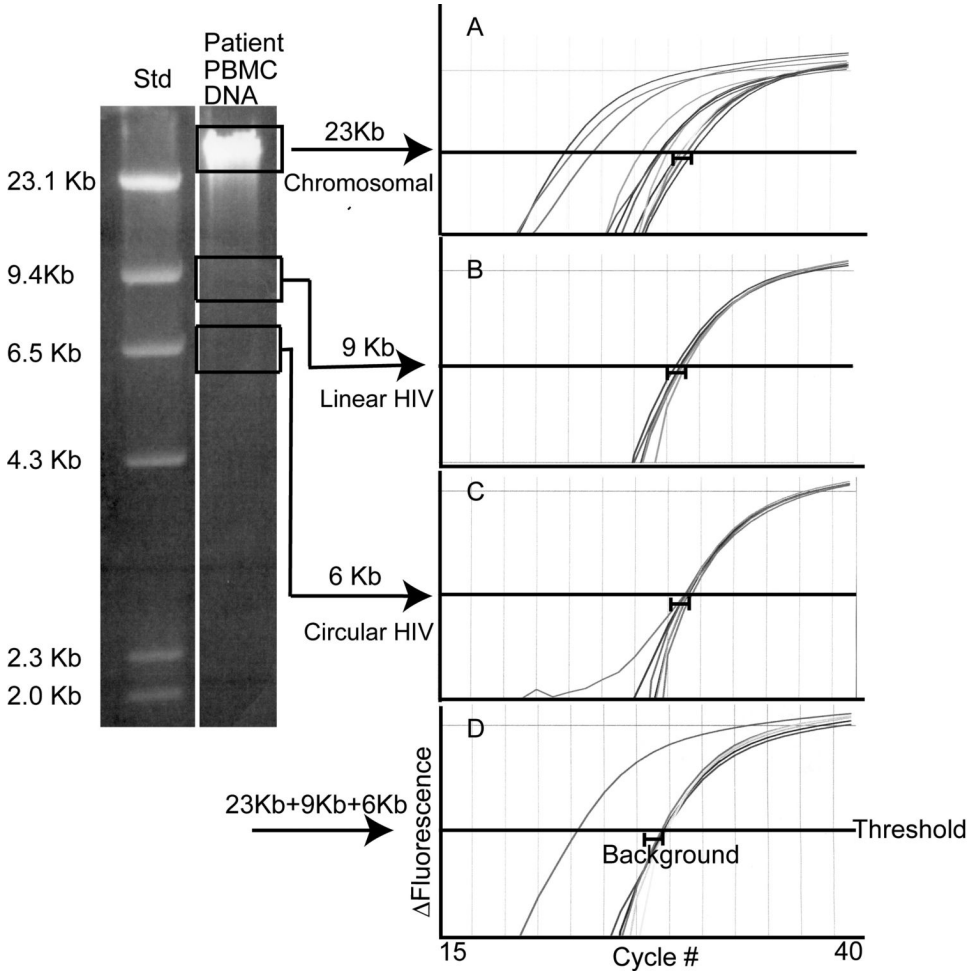

Figure 4. In a patient sample, unintegrated HIV DNA does not contribute significantly to the *Alu-gag* integration assay signal

DNA from patient PBMCs was purified and size-separated into three fractions (chromosomal, linear, and circular) by 0.7% agarose gel electrophoresis. Chromosomal DNA was ~23kb (due to fragmentation during processing), linear HIV DNA ~9kb, and circular HIV DNA ~6kb. The DNA from each fraction was extracted and resuspended in 100ul of 10 mM Tris. *Alu-gag* and *gag*-only PCR were performed on equal volumes (8.3 ul) of each fraction separately, and then on a mixture (8.3 ul of each) of the 3 fractions. The *Alu-gag* and *gag*-only curves generated from PCR are shown in plots on the right: panel (A) chromosomal, (B) linear HIV DNA, (C) circular HIV DNA, and (D) mixture of chromosomal, linear, and circular. *Alu-gag* and *gag*-only PCR were performed 6 times each on sample A and 3 times each on samples B-D (due to limited sample). *Alu-gag* and *gag*-only signals (Ct) are defined as the cycle number at which a curve crosses the threshold (0.01). A bracket (⊢⊣) indicates the range of signal obtained with *gag*-only priming. An *Alu-gag* signal is defined as positive when it is significantly different from the *gag*-only signal by Student's t-test.

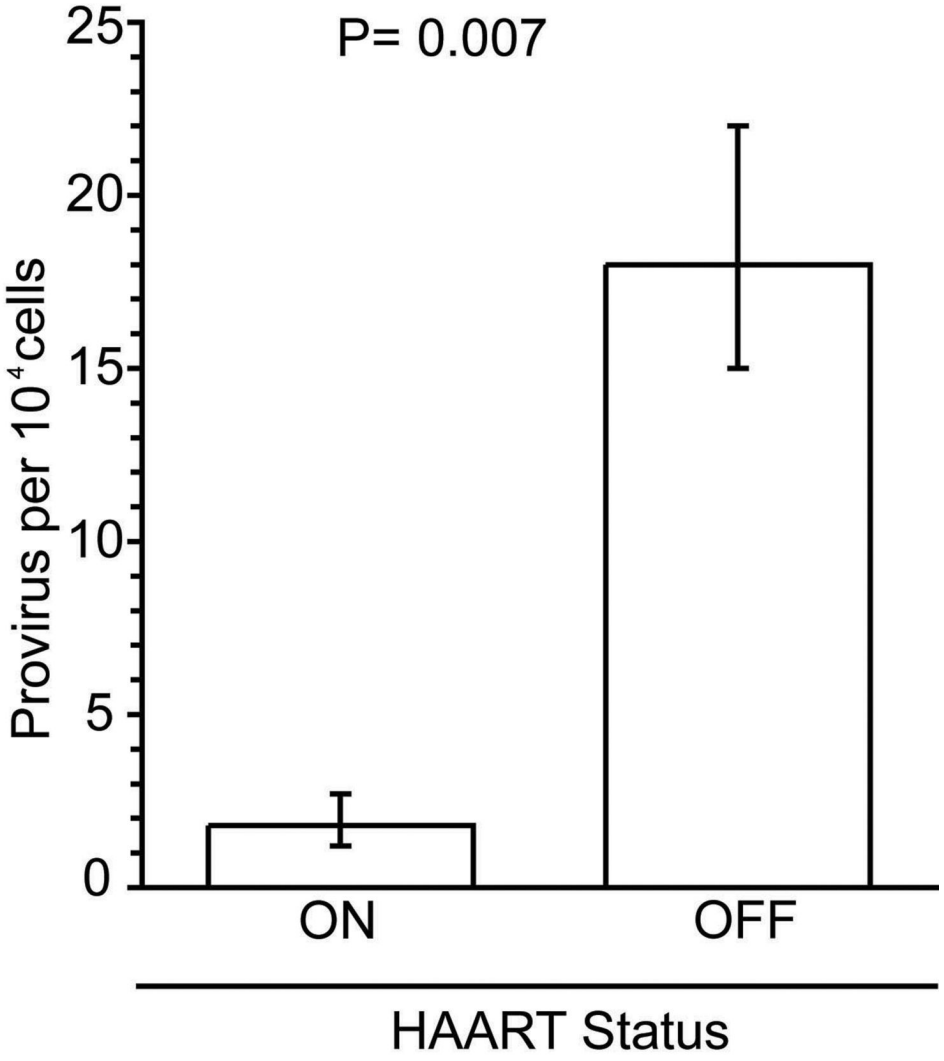

Figure 5. Patients on HAART have lower proviral loads in PBMCs than patients off HAART

The average level of provirus in patients on and off effective HAART are shown with their 95% confidence intervals and are significantly different by the Wilcoxon signed-rank test (p=0.007).

Table 1

Increasing the number of cycles in the first PCR reaction enhanced the sensitivity of the integration assay

The integration standard was diluted to 20 proviruses in 15,000 cells and then assayed repetitively with 20, 30 or 40 cycles, while the amount of enzyme, extension time and other variables were kept constant. The number of cycles performed in the first PCR reaction, the average *Alu*-*gag* and *gag*-only signal, as captured by cycle thresholds (Ct), and the difference between the signals are shown. Indicated p-values compare the *Alu*-*gag* signals to the *gag*-only signals.

Cycles	*Alu*-*gag* Ct	*gag*	Δ	P value
20	22.6	28.3	5.66	0.005
30	20.5	27.0	6.50	0.005
40	18.7	28.1	**7.41**	<0.001

Table 2

Proviral level in patients on and off HAART

The calculated number of proviruses per 10,000 cells is listed for each patient. In addition, the upper and lower bounds for 95% confidence intervals are also provided. The errors are asymmetrical because a logarithmic transformation was performed before taking averages of the ln (Ct) of the patient samples (as well as the integration standard). The p-value in the final column represents the probability that the *Alu-gag* and *gag*-only signals are not different.

HAART	Patient	Provirus per 10^4 cells	Lower 95% CI	Upper 95% CI	p-value
ON	1	0.66	0.63	0.70	2×10^{-02}
	2	2.9	2.1	4.2	7×10^{-07}
	3	2.2	1.5	3.4	1×10^{-04}
	4	3.0	2.1	4.4	3×10^{-03}
	5	2.5	1.7	3.9	2×10^{-06}
	6	0.58	0.49	0.69	2×10^{-02}
	7	0.55	0.39	0.78	3×10^{-05}
	8	0.43	0.33	0.55	2×10^{-02}
	9	3.0	1.5	6.0	3×10^{-04}
	10	1.9	1.3	2.6	6×10^{-05}
	Average	**1.8**	**1.2**	**2.7**	
OFF	11	46	38	54	2×10^{-40}
	12	19	15	25	2×10^{-15}
	13	9.1	6.8	12	2×10^{-25}
	14	6.4	4.5	8.9	2×10^{-11}
	15	27	23	32	2×10^{-13}
	Average	**18**	**15**	**22**	

Table 3

Positive *Alu-gag* signals are only detected in the chromosomal fraction of patient PBMC DNA

The average *Alu*–*gag* and *gag*-only signals were determined in Figure 4.

	Cycle number at which signal above threshold	
	***Alu-gag* (Ct)**	***gag* only (Ct)**
Chromosomal	**26.1** +/− 1.22	30.0 +/− 0.15
Linear HIV	29.6 +/− 0.11	29.9 +/− 0.07
Circular HIV	30.1 +/− 0.04	30.2 +/− 0.10
Mixture	**26.8** +/− 1.76	28.6 +/− 0.11

Table 4

Unintegrated HIV plasmid DNA contributes minimally to the *Alu-gag* signal from an integration standard

In this experiment, unintegrated HIV plasmid DNA was diluted in PBMC DNA, integration standard DNA was diluted in PBMC DNA, and unintegrated and integrated DNA were mixed in a 100:1 ratio. From these, three samples of DNA were prepared. The first sample contained 800 copies/reaction of unintegrated DNA (800 U). The second sample contained 8 copies/reaction of integration standard DNA (8 IS). The third sample was a mixture of 800 copies of unintegrated DNA and 8 integrated proviruses (800 U + 8 IS). Each sample was assayed 42 times using *Alu-gag* and *gag*-only PCR and the cycle numbers at which the *Alu-gag* and *gag*-only signals were detected above the cycle threshold are shown. Also shown are the number of proviruses calculated from the *Alu-gag* signal for each sample. The standard curve used to calculate proviruses in this figure is slightly different than the one generated in Figure 2 and used to calculate the number of proviruses for the patient samples because a different master mix was used for the experiment in Table 4. All of the other experiments described in this paper used the same master mix as was used to generate the standard curve in Figure 2.

HIV DNA copies per well	Provirus per well	Cycle number at which signal detected		p-value
		Alu-gag	*gag* only	
800 U	0	27.3	27.3	NS
8 IS	7	29.7	36.4	$\ll 0.01^{+}$
800 U + 8 IS	15	25.3	27.3	$\ll 0.01$*

Table 5

Patient Characteristics

The patient's HAART status, CD4 count, viral loads, total HIV DNA (RU5/10,000 cells +/− standard error), and the ratio of total DNA to integrated DNA are shown for each patient. Total DNA was measured using the primers and probe described in Figure 1 without the *Alu*-*gag* amplification as described in the Methods.

Patient	HAART Status	CD4 Count	Viral Load	RU5 per 10^4 cells	Provirus 10^4 cells	RU5 per Provirus
1		370	<400	12 ± 1.8	0.66	18
2		809	<50	440 ± 31	2.9	150
3		596	<50	25 ± 3.7	2.2	11
4		745	400	32 ± 3.8	3.0	11
5	ON	515	57	61 ± 12	2.5	24
6		461	<50	84 ± 4.0	0.58	140
7		903	<50	200 ± 6.1	0.55	360
8		749	<50	1.4 ± 0.13	0.43	3.3
9		506	<75	14 ± 0.32	3.0	4.7
10		322	<75	5.5 ± 0.85	1.9	2.9
			Average	**87 ± 43**	**1.8**	**72 ± 37**
11		290	unknown	310 ± 13	46	6.7
12		400	2.5×10^4	320 ± 21	19	17
13	OFF	529	6.8×10^4	87 ± 17	9.1	9.6
14		383	1.3×10^4	85 ± 14	6.4	13
15		630	8.0×10^4	610 ± 30	27	23
16		587	5.5×10^4	79 ± 15	1.5	53
			Average	**250 ± 86**	**18**	**20 ± 6.9**